Desalination and Water Treatment
www.deswater.com
doi: 10.1080/19443994.2013.787027

52 (2014) 1388–1395
February

Taylor & Francis
Taylor & Francis Group

Capacitive deionization by ordered mesoporous carbon: electrosorption isotherm, kinetics, and the effect of modification

Feng Duan[a,b,c], Yuping Li[a,b,*], Hongbin Cao[a,b,*], Yongbing Xie[a,b], Yi Zhang[a,b]

[a]*National Engineering Laboratory for Hydrometallurgical Cleaner Production Technology, Beijing 100190, China*
Tel. +86 10 82544844; Fax: +86 10 82544844/816; emails: ypli@home.ipe.ac.cn; hbcao@home.ipe.ac.cn
[b]*Key Laboratory of Green Process and Engineering, Institute of Process Engineering, Chinese Academy of Sciences, Beijing 100190, China*
[c]*University of Chinese Academy of Sciences (UCAS), Beijing 100049, China*

Received 2 December 2012; Accepted 12 March 2013

ABSTRACT

In this study, an ordered mesoporous carbon (OMC) was synthesized and investigated as electrodes for capacitive deionization (CDI). The influence of working parameters on salt removal was studied and the electrosorption isotherm and kinetics were investigated. It was found that the electrosorption process fitted both Langmuir isotherm and Freundlich isotherm, and followed pseudo-first-order kinetics. The maximum electrosorptive capacity was 10.1 mg/g at the optimized applied voltage of 1.2 V and flow rate of 40 ml/min. In order to investigate the effect of surface groups on CDI efficiency, OMC was modified by H_2O_2 solution or thermal treatment under N_2 atmosphere, without significantly changing its textural properties. X-ray photoelectron spectroscopy measurements showed that the amount of surface oxygen-containing groups was decreased and increased by the thermal and chemical treatments, respectively. CDI experiments revealed that OMC modified by H_2O_2 solution performed better than original OMC, while thermal treatment worsened the performance of OMC, probably due to the difference in their surface groups. This indicated that the CDI performance of OMC was greatly affected by the surface chemistry.

Keywords: Ordered mesoporous carbon; Capacitive deionization; Electrosorption; Modification; Surface chemistry

1. Introduction

Many regions around the world suffer from freshwater shortage, and desalination has been considered an effective solution to the problem. Conventional desalination methodologies, such as thermal distillation, reverse osmosis (RO), and electrodialysis, are usually energy intensive [1,2]. Capacitive deionization (CDI), first studied in mid-1960s, has aroused great interest in recent years due to its energy-saving characteristics [3]. It is considered to be a potential approach for the desalination of brackish water [4] and treatment of RO brine solution [5,6].

CDI behaves like an electrochemical capacitor that accumulates ions in the electrical double layers (EDL) formed on the electrode surfaces. Therefore, the electrode material is one of the most critical issues. Ideal electrode materials should meet several requirements,

*Corresponding authors.

such as large specific surface area, high electronic conductivity, chemical stability, and efficient mass transfer [3]. Carbonaceous materials, such as activated carbon (AC) [7], AC cloth [8], carbon nanotube [9], carbon aerogels [10], graphene [11], mesoporous carbons (MCs) [12,13], and composite materials [14–16] have been investigated for electrosorptive desalinaton. Among them, AC materials are intensively studied because of their high specific surface area and availability. However, EDL overlapping often occurs in the microporous carbon materials, which results in loss of electrical capacities [17]. Besides, carbon aerogels are considered as promising CDI electrode materials. They are porous materials with high specific surface area of 400–1,100 m^2/g and exceptionally high electrical conductivity of 25–100 S/cm [3]. Recently, Haro et al. [18] showed that the carbon gel was more resistant to electrochemical anodic oxidation in charge/discharge cycles than ACs. However, the manufacturing process of carbon aerogels is still time consuming, and the inner surfaces are not effectively utilized due to their dominant microporous structure [19].

It was reported that mesopores would achieve better ion accessibility and facilitate the mass transfer of ions [20]. Different synthesis strategies have been developed recently to obtain MCs with various spatial structures and surface areas, and they have been widely used in adsorption, catalysis, and electrochemical capacitors [21,22]. Zou et al. [12] firstly studied ordered mesoporous carbon (OMC) as the CDI electrode material. It showed higher desalination capacities and rates than microporous AC. Tsouris et al. [19] developed two kinds of MC electrodes and demonstrated that they removed more salts than carbon aerogel. The surface chemistry of carbon materials also affected the ion electrosorption [23]. However, few reports have studied the effects of OMC surface groups on the CDI behavior.

In this paper, we synthesized an OMC material and applied it in the CDI process. The influence of working parameters, the electrosorption isotherm, and the kinetics of OMC were investigated. Furthermore, OMC was modified by H_2O_2 solution and thermal treatment in N_2 atmosphere to investigate the effect of surface functional groups on salt removal.

2. Materials and methods

2.1. OMC preparation and modification

OMC was prepared by the evaporation-induced triconstituent co-assembly method according to the literature [21]. Briefly, 1.6 g of block copolymer F127 (Mw = 12 600, $PEO_{106}PPO_{70}PEO_{106}$) was dissolved in 8.0 g of ethanol with 1.0 g of 0.2 M HCl and stirred for 1 h at 40˚C to afford a clear solution. Next, 2.08 g of TEOS and 5.0 g of 20 wt.% resols' ethanolic solution were added in sequence. After being stirred for 2 h, the mixture was transferred into dishes. It took several hours at room temperature to evaporate ethanol and 24 h at 100˚C in an oven to thermopolymerize. The as-made product was scraped from the dishes and ground into fine powder. Calcination was carried out in a tubular furnace at 900˚C for 2 h under N_2 flow. The heating rate was 1˚C/min below 600˚C and 5˚C/min above 600˚C. Then the product was immersed in 40% HF solution for 24 h to remove silica and finally OMC was obtained.

For thermally modified OMC (denoted as OMC-N_2), it was treated at 1,000˚C for 3 h under N_2 flow. For H_2O_2 modified OMC (denoted as OMC-H_2O_2), 1.5 g OMC was treated in 80 g H_2O_2 solution (30 wt.%) at 60˚C for 30 min, and then washed with deionized water thoroughly.

2.2. Fabrication of the carbon electrodes

The OMC electrodes were fabricated according to the literature [24]. Typically, a mixture was prepared by mixing carbon (80 wt.%), acetylene black (10 wt.%) and poly(vinylidene fluoride) (PVDF) (10 wt.%). N,N-dimethylacetamide was added to dissolve PVDF under stirring. The slurry was then cast onto a graphite sheet which was used as current collector. The size of the electrode was about 35 mm long and 35 mm wide. Finally, it was dried at 150˚C for 2 h to remove all organic solvents.

2.3. Characterization

Transmission electron microscopy (TEM) measurement was conducted using a JEM 2010 microscope (JEOL, Japan). X-ray photoelectron spectroscopy (XPS) analysis was performed with a VG Scientific ESCALAB 250Xi spectrometer using monochromatic Al Kα radiation. Nitrogen sorption isotherms were measured at 77 K with an automated gas sorption analyzer (Quantachrome autosorb iQ). Before measuring, the samples were degassed under vacuum at 200˚C for 8 h. The specific surface areas (S_{BET}) and pore size distributions (PSD) of OMCs were obtained by the Brunauer–Emmett–Teller (BET) method and the Barrett–Joyner–Halenda model, respectively. The total pore volumes (V_t) were estimated from the amount adsorbed at a relative pressure of about 0.990.

To investigate the electrochemical performance of OMCs, cyclic voltammetry (CV) was performed using a three-electrode system in the Autolab PGSTAT302 N instrument (Metrohm). The working electrode, with a size of 10 mm × 10 mm, was prepared using the method mentioned above. A platinum sheet electrode and a saturated calomel electrode (SCE) were used as the counter and reference electrodes, respectively. CV was measured at the sweep rate of 25–50 mV/s in the potential range of −0.6 to 0.6 V (vs. SCE) in 0.2 mol/L NaCl solution at 25°C. The specific capacitances were calculated from CV curves using Eq. (1):

$$C_m = \frac{\int_{V_0}^{V_t} |I| dV}{2 \times s \times m \times \Delta V} \quad (1)$$

where C_m (F/g) is the specific capacitance, I (A) is the current, V_0 and V_t (V) are the start and the end potentials, respectively, ΔV (V) is the potential difference between V_0 and V_t, s (mV/s) is the scan rate, and m (g) is the weight of carbon in the electrode.

2.4. Desalination experiments

The schematic of the CDI apparatus is shown in Fig. 1. Two electrodes were placed face to face, separated by a hollow rubber gasket. The gap between the electrodes was kept ~6 mm. A flow channel was created by punching a 1 cm-diameter hole in the electrodes and the end plates. The apparatus was held together by threaded rods which were insulated from the carbon electrodes.

Batch mode experiments were conducted by continuously recycling the NaCl solution with a peristaltic pump. The potential was applied by a direct-current power supply. Before applying the potential, the solution was recycled for ~30 min until the conductivity was stable. To optimize the operational conditions, experiments were carried out at the applied voltage of 0.8–2.0 V and flow rate of 10–70 ml/min, and NaCl concentration was 25 mg/L. The total volume was maintained at 100 mL and the temperature was kept at (25 ± 1)°C. The conductivity and pH of the effluents were measured by a conductivity meter (Orion 3-Star, Thermo Fisher Scientific Inc.) and pH meter (FE30, Mettler Toledo), respectively. The relationship between the conductivity and concentration was calibrated before the desalination experiments. The electrosorptive capacity was calculated according to the following formula:

$$q = (C_0 - C) \times V/m \quad (2)$$

where q (mg/g) is electrosorptive capacity, C_0 and C (mg/L) represent the initial and final concentration, respectively, V (L) is the solution volume, and m (g) is the mass of carbon material.

3. Results and discussion

3.1. Characterization of OMC and modified OMCs

From the TEM image of OMC in Fig. 2, well-ordered channels were clearly seen, indicating mesopore structure in hexagonal arrays [21]. The pore size was estimated to be ~5 nm. The N_2 sorption isotherms and PSD curves of OMCs are shown in Fig. 3 and their textural properties are summarized in Table 1. All the three OMCs exhibited type-IV isotherm with H2 hysteresis, which represents narrow mesopore distributions. Furthermore, they showed similar surface area, total pore volume, and pore size, which indicated that the textural properties of OMC were not changed significantly by the thermal and chemical

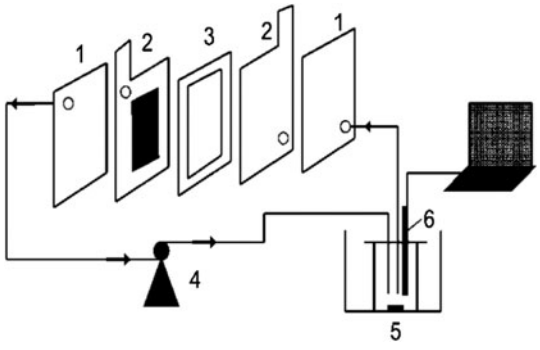

Fig. 1. Schematic of CDI experiment ((1) end plate; (2) carbon electrode; (3) hollow rubber gasket; (4) peristaltic pump; (5) magnetic stirrer; (6) conductivity/pH meter).

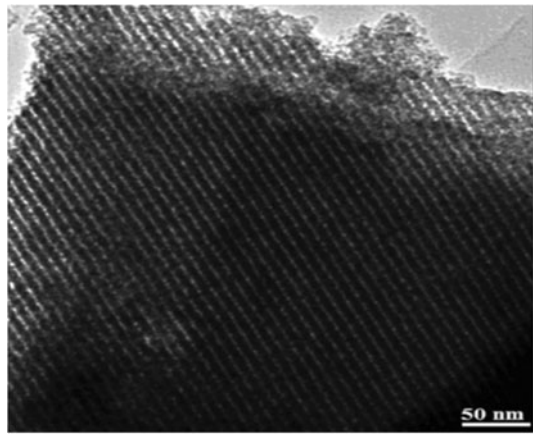

Fig. 2. TEM image of OMC viewed from the [1 1 0] direction.

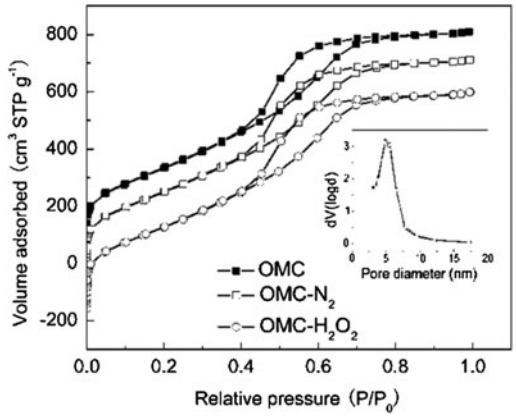

Fig. 3. The N_2 sorption isotherms and PSD curves (inset figure) of OMCs (the isotherms of OMC-N_2 and OMC-H_2O_2 are offset vertically by 100 and 200 cm^3/g, respectively).

Table 1
Textural properties of OMC and modified OMCs

Sample	S_{BET} (m^2/g)	V_t (cm^3/g)	Pore size (nm)
OMC	1,232	1.252	4.9
OMC-N_2	1,270	1.255	4.9
OMC-H_2O_2	1,206	1.237	4.9

treatments. Fig. 4 depicts the full range XPS spectra of OMCs. The elements C and O were mainly indentified on the carbon surface. From Table 2, the surface oxygen concentration of OMC was 5.0%, while that of OMC-N_2 decreased to 4.4% and OMC-H_2O_2 increased to 7.3%. Therefore, surface oxides became less when OMC was treated thermally in N_2 atmosphere, while more surface oxides would be created by H_2O_2 treatment.

3.2. Electrochemical performance of OMCs

The CV behaviors of OMCs were measured, as seen in Fig. 5. The specific capacitances at different sweep rates could be calculated from the CV curves using Eq. (1), and the order was always OMC-H_2O_2 > OMC > OMC-N_2. For example, OMC showed specific capacitance of 43.8 F/g at 50 mV/s, while that of OMC-H_2O_2 and OMC-N_2 were 50.6 and 40.4 F/g at the same sweep rate. It seemed that the H_2O_2 treatment increased the capacitance of OMC while the thermal treatment decreased it, probably due to the increase and decrease of oxygen functional groups, respectively, as indicated by the XPS results. Because OMC-H_2O_2 showed the highest capacitance, it is likely to perform the best when used for CDI electrodes.

3.3. Effect of working parameters on the CDI performance of OMC electrodes

The working parameters of CDI behavior with OMC electrodes, including applied voltage and flow rate, were systematically investigated. Fig. 6(A) shows the electrosorption performance at different applied voltages at flow rate of 40 ml/min. The electrosorptive capacity increased as the applied voltage increased. With the increase in voltage from 0.8 to 2.0 V, the amount of salt removal increased from 2.3 to 6.1 mg/g after charging for 300 min. This is probably because higher voltage leads to larger electrostatic attractions. However, Faradaic reactions are more likely to occur when the voltage is higher; thus, the current efficiency is decreased. The inset image in Fig. 6(a) shows pH values at determined time. The pH change at 1.6 or 2.0 V was more dramatic than that at 0.8 or 1.2 V. As the voltage of 1.2 V ensured a relatively high desalination capacity as well as few electrochemical reactions, it was selected in the subsequent experiments. Fig. 6 (b) depicts the CDI behavior at different flow rates at 1.2 V. The electrosorption rate is too slow at a flow rate of 10 ml/min. When the flow rate was increased, the ion removal rate improved, probably because a high flow rate facilitated the ion transport between the solution and the pores of electrodes. However, a too high flow rate like 70 ml/min was not beneficial to electrosorption as it probably resulted in solution turbulence. The best desalination performance was obtained at 40 ml/min.

3.4. Electrosorption isotherm

To obtain the electrosorption isotherm of OMC, experiments were carried out in NaCl solutions of 25–500 mg/L, with applied potential of 1.2 V, flow rate of 40 ml/min, and each electrode of ~0.15 g. The equilibrium stage was determined when the conductivity was not changed for almost 1 h. Langmuir (Eq. (3)) and Freundlich (Eq. (4)) isotherms were employed to fit the experimental data (Fig. 7).

$$q_e = \frac{q_m K_L C_e}{1 + K_L C_e} \quad (3)$$

$$q_e = K_F C_e^{1/n} \quad (4)$$

where q_e (mg/g) is the equilibrium electrosorptive capacity calculated according to Eq. (2) and q_m (mg/g) is the maximum electrosorptive capacity. C_e (mg/L) is the equilibrium concentration of NaCl, K_L (L/mg) is a constant related to adsorption heat, and K_F (L/g) and

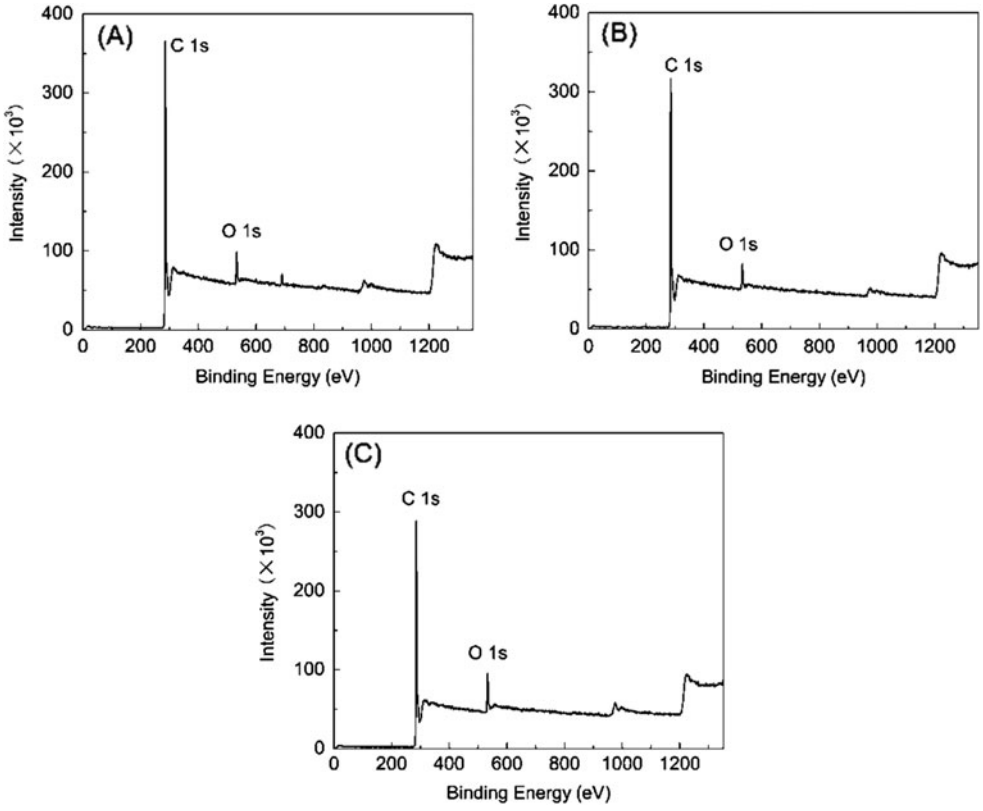

Fig. 4. Full range XPS spectra of (A) OMC, (B) OMC-N_2, and (C) OMC-H_2O_2.

Table 2
Surface concentrations (%) of C and O species of OMCs

Sample	OMC	OMC-N_2	OMC-H_2O_2
C	95.0	95.6	92.7
O	5.0	4.4	7.3

n are constants of Freundlich isotherm. Table 3 shows the determined parameters of different isotherms.

It seemed that both isotherms correlated well with the experimental data of OMC according to the correlation coefficient (R^2). The simulated value of q_m in the Langmuir isotherm was 10.1 mg/g corresponding to the maximum monolayer coverage. The value of n in the Freundlich isotherm was higher than 1, which indicated that the process of ion electrosorption on OMC electrodes was favorable [25].

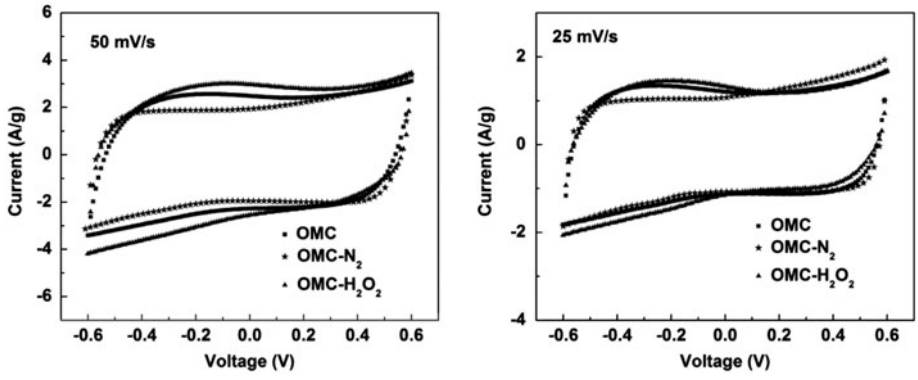

Fig. 5. Cyclic voltammograms of OMCs at different sweep rates in 0.2 mol/L NaCl electrolyte.

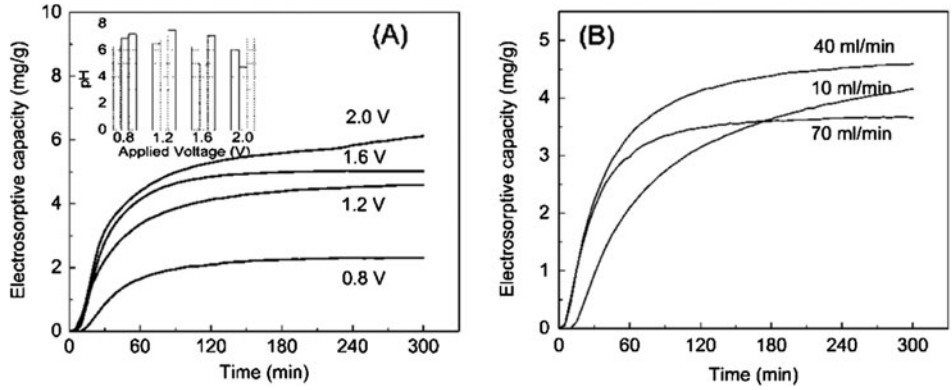

Fig. 6. The CDI performance of OMC at different: (A) applied voltages, and (B) flow rates. The inset image in figure (A) shows the pH values when a certain voltage was applied for 0, 10, and 300 min (from left to right), respectively. The NaCl concentration is 25 mg/L and each electrode is ~0.15 g.

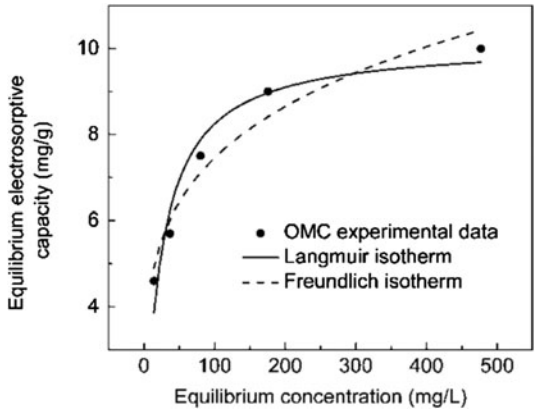

Fig. 7. The electrosorption isotherm of OMC.

Table 3
The parameters of Langmuir and Freundlich isotherms for OMC

Isotherm	Equation	Parameters	Value
Langmuir	$q_e = \frac{q_m K_L C_e}{1 + K_L C_e}$	q_m	10.1
		K_L	0.043
		R^2	0.946
Freundlich		K_F	2.77
	$q_e = K_F C_e^{1/n}$		
		n	4.65
		R^2	0.956

3.5. Electrosorption kinetics

The electrosorption kinetics was analyzed by the pseudo-first-order (Eq. (5)) and pseudo-second-order (Eq. (6)) adsorption kinetics model, and the results are shown in Table 4.

$$\frac{dq}{dt} = k_1(q_e - q) \tag{5}$$

$$\frac{dq}{dt} = k_2(q_e - q)^2 \tag{6}$$

where k_1 (min^{-1}) and k_2 ($g\,mg^{-1}\,min^{-1}$) are the pseudo-first-order and the pseudo-second-order adsorption rate constant, respectively, q_e and q (mg/g) are the amount of NaCl adsorbed at equilibrium and time t (min), respectively.

It seemed that the pseudo-first-order kinetics fitted the electrosorption process better than the pseudo-second-order kinetics according to R^2. The equilibrium electrosorptive capacity and rate constant increased when the salt concentration increased from 25 to 500 mg/L. This is probably attributed to the increase in OMC capacitance with the increase of salt concentration.

3.6. Comparison of the CDI performance of OMCs and modified OMCs

To investigate the effects of surface modifications of OMC on the CDI behavior, the three OMCs were studied for comparison. The experiments were conducted using NaCl solution of 100 mg/L, voltage of 1.2 V, flow rate of 40 ml/min, and each electrode of ~0.23 g. As shown in Fig. 8, OMC-H_2O_2 performed better than OMC, while OMC-N_2 performed worse, which were in accordance with the CV measurement results. The electrosorptive capacities were 7.6, 6.1, and 4.2 mg/g for OMC-H_2O_2, OMC, and OMC-N_2, respectively. The ion

Table 4
The parameters of pseudo-first-order and pseudo-second-order kinetics for OMC with different NaCl concentrations

C_0 (mg/L)	Pseudo-first-order			Pseudo-second-order		
	q_e (mg/g)	k_1 (min^{-1})	R^2	q_e (mg/g)	k_2 (g/mg/min)	R^2
25	4.5	0.0214	0.993	5.3	0.0048	0.982
50	5.7	0.0336	0.991	6.3	0.0075	0.958
100	7.6	0.0465	0.997	8.2	0.0092	0.961
200	9.0	0.0582	0.998	9.6	0.0107	0.967
500	9.9	0.0855	0.982	10.6	0.0137	0.995

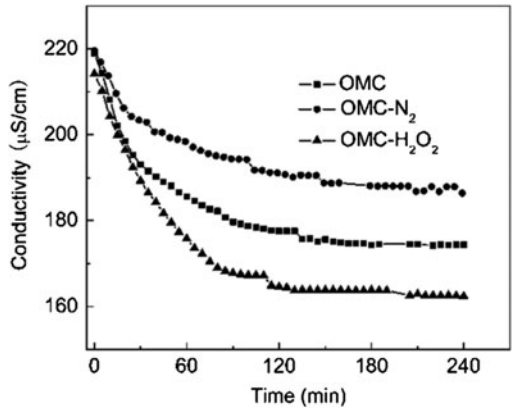

Fig. 8. The desalination performance of three OMCs.

electrosorption behavior was mainly dependent on the surface area, PSD, and surface chemistry of the carbon materials [12,26]. Because all the OMCs showed similar surface area and pore size, the surface functional groups greatly affected the CDI performance. The hydrophilicity of OMC can be improved by increasing the surface oxygen groups; thus the electrodes will be fully wetted, which is beneficial to the adsorption of ions [8]. Besides, the surface groups provide the binding sites for possible ion exchange or electrochemical ion exchange [26]. Therefore, it is an effective way to increase the CDI removal efficiency of OMC by creating more surface oxides.

4. Conclusion

In this paper, we investigated the electrosorptive desalination behavior of OMC. The suitable applied voltage was 1.2 V and suitable flow rate was 40 ml/min. Both the Langmuir isotherm and Freundlich isotherm correlated well with the experimental data. The maximum electrosorptive capacity was 10.1 mg/g at the optimum working parameters. Besides, the pseudo-first-order kinetics fitted the CDI process better than the pseudo-second-order kinetics. The H_2O_2 treatment of OMC facilitated ion electrosorption, while the thermal treatment under N_2 atmosphere negatively affected it. The surface groups improved the hydrophilicity and provided the binding sites for possible ion exchange, which were favorable to the capacitive desalination.

Acknowledgment

The authors greatly appreciate the financial support from the National Natural Science Foundation of China (Grant No. 20607023 and No. 21177130).

References

[1] T.J. Welgemoed, C.F. Schutte, Capacitive Delonization Technology (TM): An alternative desalination solution, Desalination 183 (2005) 327–340.
[2] M.A. Anderson, A.L. Cudero, J. Palma, Capacitive deionization as an electrochemical means of saving energy and delivering clean water. Comparison to present desalination practices: Will it compete? Electrochim. Acta 55 (2010) 3845–3856.
[3] Y. Oren, Capacitive delonization (CDI) for desalination and water treatment–past, present and future (a review), Desalination 228 (2008) 10–29.
[4] E. Avraham, Y. Bouhadana, A. Soffer, D. Aurbach, Limitation of charge efficiency in capacitive deionization I.on the behavior of single activated carbon, J. Electrochem. Soc. 156 (2009) 95–99.
[5] N. Afrasiabi, E. Shahbazali, RO brine treatment and disposal methods, Desalin. Water Treat. 35 (2011) 39–53.
[6] G. Tao, B. Viswanath, K. Kekre, L.Y. Lee, H.Y. Ng, S.L. Ong, H. Seah, RO brine treatment and recovery by biological activated carbon and capacitive deionization process, Water Sci. Technol. 64 (2011) 77.
[7] Z.L. Chen, C.Y. Song, X.W. Sun, H.F. Guo, G.D. Zhu, Kinetic and isotherm studies on the electrosorption of NaCl from aqueous solutions by activated carbon electrodes, Desalination 267 (2011) 239–243.
[8] S.-J. Seo, H. Jeon, J.K. Lee, G.-Y. Kim, D. Park, H. Nojima, J. Lee, S.-H. Moon, Investigation on removal of hardness ions by capacitive deionization (CDI) for water softening applications, Water Res. 44 (2010) 2267–2275.
[9] X.Z. Wang, M.G. Li, Y.W. Chen, R.M. Cheng, S.M. Huang, L.K. Pan, Z. Sun, Electrosorption of ions from aqueous solutions with carbon nanotubes and nanofibers composite film electrodes, Appl. Phys. Lett. 89 (2006) 0531271–0531273.
[10] C.J. Gabelich, T.D. Tran, I.H. Suffet, Electrosorption of inorganic salts from aqueous solution using carbon aerogels, Environ. Sci. Technol. 36 (2002) 3010–3019.
[11] H.B. Li, L.D. Zou, L.K. Pan, Z. Sun, Novel graphene-like electrodes for capacitive deionization, Environ. Sci. Technol. 44 (2010) 8692–8697.
[12] L.D. Zou, L.X. Li, H.H. Song, G. Morris, Using mesoporous carbon electrodes for brackish water desalination, Water Res. 42 (2008) 2340–2348.

[13] L.X. Li, L.D. Zou, H.H. Song, G. Morris, Ordered mesoporous carbons synthesized by a modified sol-gel process for electrosorptive removal of sodium chloride, Carbon 47 (2009) 775–781.
[14] Z. Peng, D.S. Zhang, L.Y. Shi, T.T. Yan, High performance ordered mesoporous carbon/carbon nanotube composite electrodes for capacitive deionization, J. Mater. Chem. 22 (2012) 6603–6612.
[15] D.S. Zhang, T.T. Yan, L.Y. Shi, Z. Peng, X.R. Wen, J.P. Zhang, Enhanced capacitive deionization performance of graphene/carbon nanotube composites, J. Mater. Chem. 22 (2012) 14696–14704.
[16] D.K. Kohli, R. Singh, M.K. Singh, A. Singh, R.K. Khardekar, P. Ram Sankar, P. Tiwari, P.K. Gupta, Study of carbon aerogel-activated carbon composite electrodes for capacitive deionization application, Desalin. Water Treat. 49 (2012) 130–135.
[17] K.L. Yang, T.Y. Ying, S. Yiacoumi, C. Tsouris, E.S. Vittoratos, Electrosorption of ions from aqueous solutions by carbon aerogel: An electrical double-layer model, Langmuir 17 (2001) 1961–1969.
[18] M. Haro, G. Rasines, C. Macias, C.O. Ania, Stability of a carbon gel electrode when used for the electro-assisted removal of ions from brackish water, Carbon 49 (2011) 3723–3730.
[19] C. Tsouris, R. Mayes, J. Kiggans, K. Sharma, S. Yiacoumi, D. Depaoli, S. Dai, Mesoporous carbon for capacitive deionization of saline water, Environ. Sci. Technol. 45 (2011) 10243–10249.
[20] S. Nadakatti, M. Tendulkar, M. Kadam, Use of mesoporous conductive carbon black to enhance performance of activated carbon electrodes in capacitive deionization technology, Desalination 268 (2011) 182–188.
[21] R.L. Liu, Y.F. Shi, Y. Wan, Y. Meng, F.Q. Zhang, D. Gu, Z.X. Chen, B. Tu, D.Y. Zhao, Triconstituent co-assembly to ordered mesostructured polymer-silica and carbon-silica nanocomposites and large-pore mesoporous carbons with high surface areas, J. Am. Chem. Soc. 128 (2006) 11652–11662.
[22] C.D. Liang, Z.J. Li, S. Dai, Mesoporous carbon materials: Synthesis and modification, Angew. Chem. Int. Ed. 47 (2008) 3696–3717.
[23] I. Villar, S. Roldan, V. Ruiz, M. Granda, C. Blanco, R. Menendez, R. Santamaria, Capacitive deionization of NaCl solutions with modified activated carbon electrodes, Energy Fuels 24 (2010) 3329–3333.
[24] J.H. Choi, Fabrication of a carbon electrode using activated carbon powder and application to the capacitive deionization process, Sep. Purif. Technol. 70 (2010) 362–366.
[25] H.B. Li, L. Zou, L.K. Pan, Z. Sun, Using graphene nano-flakes as electrodes to remove ferric ions by capacitive deionization, Sep. Purif. Technol. 75 (2010) 8–14.
[26] H. Oda, Y. Nakagawa, Removal of ionic substances from dilute solution using activated carbon electrodes, Carbon 41 (2003) 1037–1047.